ECS Transactions, 41 (1) 1969-1977 (2011)
10.1149/1.3635726 ©The Electrochemical Society

# Anode Catalysts for the Direct Dimethyl Ether Fuel Cell

Qing Li, Gang Wu, Christina M. Johnston, and Piotr Zelenay

Materials Physics and Applications Division, Los Alamos National Laboratory
Los Alamos, New Mexico 87545, USA

For the last decade, dimethyl ether (DME) has been considered a promising alternative fuel for direct fuel cells because of several advantages over methanol. In this work, PtRu catalysts with a wide range of Pt-to-Ru ratios were screened for the direct DME fuel cell (DDMEFC) performance for the first time. Overall, $Pt_{50}Ru_{50}$ performs best in the high and middle voltage ranges, whereas $Pt_{80}Ru_{20}$ performs best at low voltages. A maximum power density of 0.10 W/cm$^2$ is achieved at a current density of 0.37 A/cm$^2$. In spite of using gaseous DME feed, the measured performance exceeds the best previously published results. The anode activity and fuel crossover of a DDMEFC were investigated in this work and compared to those of a DMFC. The adsorption and electro-oxidation of DME on Pt black catalyst were also studied in half-cell electrochemical measurements.

## Introduction

Recently, the rapid development of powerful portable devices, such as mobile phones, notebooks and digital cameras has significantly increased the demand for high-output power sources. Although commercial power sources (i.e., lithium ion and metal hydride secondary batteries) have provided relatively sufficient energy for portable devices up to now, these batteries cannot increase the energy output without increasing the total weight of the devices and consequently a new alternative power source would be highly desirable in the near future (1). Direct-feed fuel cells, especially direct methanol fuel cells (DMFCs), offer promise for portable power applications due to the high energy density of liquid fuels, and because fuel reforming and anode humidification are not required. In spite of an impressive progress in the last two decades, several inherent problems hinder the commercialization of the DMFC, including the low rate of methanol electro-oxidation, methanol and anode catalyst (i.e., ruthenium) crossover to the cathode, and safety concerns about the fuel itself.

Dimethyl ether (DME), a widely used gas for aerosol propellants, solvents and coolants, has been studied for the last decade as an alternative fuel for portable-power use. Some advantages for its implementation in fuel cells are the following: (i) when oxidized to $CO_2$, one DME molecule releases 12 electrons in the reaction

$$CH_3OCH_3 + 3H_2O \rightarrow 2CO_2 + 12H^+ + 12e^- \quad [1]$$

which results in reduced theoretical fuel consumption compared to methanol (6 e$^-$); hydrogen (2 e$^-$) (based on lower heating values, DME has higher energy density than

methanol, 8.2 *vs.* 6.1 kWh/kg); (ii) lack of a C-C bond makes complete electro-oxidation more feasible with a minimum kinetic energy loss (2); (iii) perhaps due to a lower DME dipole moment, the fuel crossover is generally less than that of methanol and with a relatively lesser effect on the cathode performance (2, 3); and (iv) DME is less toxic than methanol and can be conveniently stored and transported using existing infrastructure and technologies developed for propane and butane.

A summary of the direct DME fuel cell (DDMEFC) development can be found in a recent review by Serov *et al.* (1). Although DME is less electrochemically active than methanol at 50°C (4), Müller *et al.* (2) have demonstrated that performance of a DDMEFC under 5 atm at 130°C is nearly identical to that of a DMFC. This suggests that the temperature dependence of DME oxidation is much stronger than that of methanol, making DME more attractive as a fuel at elevated temperatures. As demonstrated in previous reports, one of the intermediate products of DME electrooxidation is CO. Similarly to methanol, bimetallic platinum-based alloys that mitigate the poisonous effect of CO on Pt materials have also been studied in the electro-oxidation of DME. Liu *et al.* (5) have investigated the electro-oxidation of DME on PtMe/Cs (Me = Ru, Sn, Mo, Cr, Ni, Co, and W) and Pt/C electrocatalysts and demonstrated that the PtRu/C shows the best electrocatalytic activity and the highest tolerance to the poisonous species in the low overpotential range (< 0.55 V, 50°C). PtRu has also been compared with Pt and PtPd using an MEA evaluation by Yoo *et al.* (6). PtRu/C and PtSn/C with different atomic ratios have been studies by Kerangueven *et al.* (7). For further optimization of the DDMEFC performance, the influence of several fuel cell conditions has been investigated recently. The dependence of MEA performance on the membrane thickness has been studied by Mench *et al.* (8). Optimization of performance by varying conditions such as temperature, backpressure, feed type, flow field types and addition of a second fuel to DME has been studied in the series of works by Cho and co-workers (5, 6, 9, 10). Yin *et al.* (11-13) has investigated the effects of the composition of catalyst layers and gas diffusion layers (GDLs) on the DDMEFC performance.

To date, the mechanism of DME oxidation has not been fully clarified, hampering the design of more advanced catalysts for the DDMEFC anode. Traces of methanol and formic acid were detected in the DDMEFC anode exhaust by Müller *et al.* (2) and by Tsutsumi *et al.* (14), respectively, and different electrooxidation mechanisms for DME were proposed. Recently, *in situ* infrared (IR) spectroscopy experiments have been carried out by several groups (15-18) to identify the intermediate and reaction products of DME adsorption and electrooxidation at platinum electrodes. Several dominant DME adsorption species, such as $(CH_3OCH_2–)_{ad}$, $CO_L$ (linearly bonded CO), $CO_B$ (bridge bonded CO), $(–CHO)_{ad}$ and $(–OCH_3)_{ad}$, have been detected by nearly every group. However, additional intermediates have also been reported by some groups, probably due to the dissimilarity of experimental conditions.

In this paper, we present the screening of unsupported PtRu catalysts with a wide range of composition at the DDMEFC anode for the first time. Fuel cell performance, anode activity and fuel crossover of a DDMEFC are evaluated and compared with a DMFC at a low temperature. Half-cell electrochemical measurements were also performed to investigate the DME adsorption and electro-oxidation at Pt black catalyst.

## Experimental

### MEA Preparation

Membrane electrode assemblies (MEAs) were fabricated from acid form membranes (Nafion® 117) and catalyst inks. Unsupported PtRu ($Pt_{90}Ru_{10}$, $Pt_{80}Ru_{20}$, $Pt_{67}Ru_{33}$, $Pt_{50}Ru_{50}$, $Pt_{40}Ru_{60}$ and $Pt_{34}Ru_{66}$, Johnson Matthey) and Pt (Johnson Matthey) catalysts were used for anode and cathode catalyst layers, respectively. Catalyst inks were prepared by ultrasonically mixing appropriate amounts of catalyst powders with de-ionized water (Millipore, 18 MΩ cm) and 5% Nafion® solution (Ion Power, Inc.) for 90 seconds. Then, the catalyst ink was directly painted onto the membrane at 75°C and dried for 30 min. The catalyst loadings were 6 and 4 mg/cm$^2$ for anode and cathode, respectively. Carbon paper of the type GDL 25 BC and GDL 25 BL (SGL Group) were used at the anode and cathode, respectively. The geometric active cell area was 5 cm$^2$.

### Fuel Cell Testing

DDMEFC testing was carried out using a commercial fuel cell test system (Fuel Cell Technologies, Inc.) with a single cell. The fabricated MEA was sandwiched between two graphite serpentine flow channels, and finally the assembly was held together with two aluminum backing plates using a set of eight retaining bolts positioned around the periphery of the cell. The cell was operated at 80°C. DME gas (99% purity, Aldrich) and air were initially supplied to the humidity bottles (DME: 85°C, Air: 90°C) and then fed to the anode and cathode compartments, respectively. Before collecting the data from the DDMEFC, the electrochemical behavior of the hydrogen/air fuel cell and the DMFC were assessed. Hydrogen/air fuel cell performance was recorded after 2 h of break-in at 0.7 V, under fully humidified and back-pressurized (ca. 20 psig) conditions. For DMFC tests, methanol (0.5 M) was pumped through the anode flow field at a flow rate of 1.8 mL/min using a high pressure liquid chromatography pump (Shimadzu LC-10AS), and humidified air was supplied to the cathode at a flow rate of 500 sccm (standard cubic centimeters per minute) at ambient pressure.

### Electrochemical Measurements

For the electrochemical measurements, Pt black powders (Johnson Matthey) were ultrasonically mixed with appropriate amounts of de-ionized water and 5% Nafion® solution (Ion Power, Inc.) for 30 min and then 15 microliters of the dispersion was quantitatively transferred to the surface of a polished glassy carbon electrode with a geometric area of 0.196 cm$^2$. Consequently, the loading of Pt was 60 μg/cm$^2$ based on the geometric electrode area. The electrochemical measurements were performed using a CHI Electrochemical Station (Model 750b) in a conventional three-electrode cell. The forming gas (6% $H_2$/balance $N_2$) was bubbled through an electrolyte solution containing a platinized platinum electrode and was used as a reference electrode. All measured potentials were later converted to the reversible hydrogen electrode (RHE) scale. A graphite rod was used a counter electrode. The electrode was electrochemically cleaned under a nitrogen atmosphere in the electrolyte between 0.05 V and 1.2 V at a scan rate of 500 mVs$^{-1}$ until a steady-state voltammogram was obtained. The DME gas was bubbled through the electrolyte at ambient pressure for ca. 3 min without further purification to form a saturated solution. The saturation concentrations of DME in 0.5 M $H_2SO_4$ and

0.1 M $HClO_4$ solution at 20°C were found to be 1.65 M (2) and 1.05 M (15), respectively. Cyclic voltammetry and DME stripping experiments were carried out after these pretreatments. All the experiments were carried out at room temperature.

## Results and Discussion

### Effects of the DME Flow Rate and Anode Backpressure

In this experiment, the performance of the DDMEFC was tested by varying the flow rate of humidified DME gas and the anode backpressure. **Figure 1a** and **1b** show the influence of the DME flow rate and the anode backpressure on the DDMEFC performance, respectively. It is obvious that the flow rate change from 40 to 140 sccm does not have much impact on the DDMEFC performance. However, the performance is enhanced noticeably with the increase of anode backpressure from 10 to 30 psig and this result is in good agreement with previous reports (7, 10). In the present research, DME is fed in gas phase into the fuel cell with water vapor at 85 °C and the amount of water supplied is insufficient for complete electro-oxidation of DME (The mole ratio of DME and water in complete oxidation reaction of DME is 1:3, but in the gas feed conditions this ratio is 1:2.2, (10)). Therefore, replacing the current DME gas feed to liquid feed may be a feasible way of improving the DDMEFC performance.

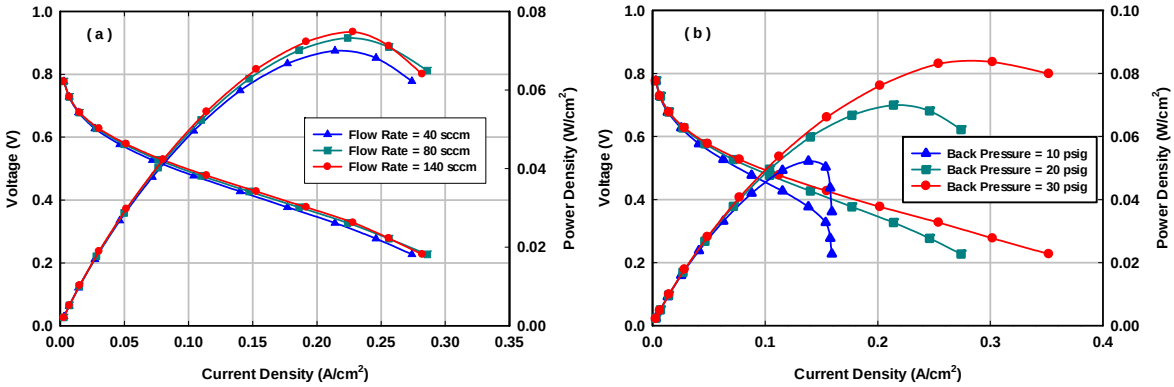


**Figure 1.** Effects of (a) the flow rate of DME gas and (b) the anode backpressure on cell voltage and power density *vs.* current density curves. Anode: 6 mg/cm$^2$ $Pt_{50}Ru_{50}$ black; cathode: 4 mg/cm$^2$ Pt black, 20 psig, 500 sccm air; membrane: Nafion® 117; cell temperature: 80°C.

### DDMEFC Performance

PtRu catalysts with a wide range of Pt-to-Ru ratios were screened for the DDMEFC performance for the first time (**Figure 2**). In general, $Pt_{50}Ru_{50}$ shows the best overall performance in the high and middle voltage ranges, and $Pt_{80}Ru_{20}$ performs the best at low voltages (high anode potentials). A maximum power density of 0.10 W/cm$^2$ was achieved at a current density of 0.37 A/cm$^2$. In spite of using gaseous DME feed, the measured performance still exceeds the best previously published results (10). Nevertheless, a DMFC still outperforms a DDMEFC under the existing low-temperature experimental conditions (data not shown).

DDMEFC current densities as a function of Pt content in the PtRu black catalyst at different fuel cell voltages are given in **Figure 3**. The data indicate that Ru-rich catalysts offer better performance at high fuel cell voltages (kinetic region of the anode), whereas Pt-rich catalysts perform better at low voltages (near peak power). In addition, Figure 2 demonstrates that Ru-rich catalysts result in a higher open cell voltage (OCV). This effect can be explained by a bi-functional mechanism of DME oxidation, according to which Ru activates water molecules to form OH species at lower potentials, therefore favoring CO oxidation and reducing the degree of poisoning of Pt sites. However, initial DME adsorption at Pt requires several adjacent sites, and the existence of the second metal may dilute the Pt adsorption sites and inhibit the formation of the intermediate adsorption species (5, 7). (Such arguments are analogous to those offered to explain the optimal PtRu composition for methanol oxidation (19).) This interpretation can be corroborated by Liu *et al.*'s work (5) which found that in spite of decreasing the onset potential of DME electrooxidation, Ru actually increases the activation energy of the DME electro-oxidation reaction: PtRu/C (57 kJ/mol) > Pt/C (46 kJ/mol). Finding the ideal compromise between the need for sufficiently large Pt clusters for DME molecule dehydrogenation and the presence of a surface oxidant, such as Ru, to remove surface CO is likely the key to successful development of a viable DME oxidation electrocatalyst. Balancing Pt and Ru sites for different functions is also required for methanol oxidation catalysts (19), but the optimal composition for DME oxidation strongly depends on potential (unlike for methanol oxidation), making the ultimate catalyst selection more complicated.

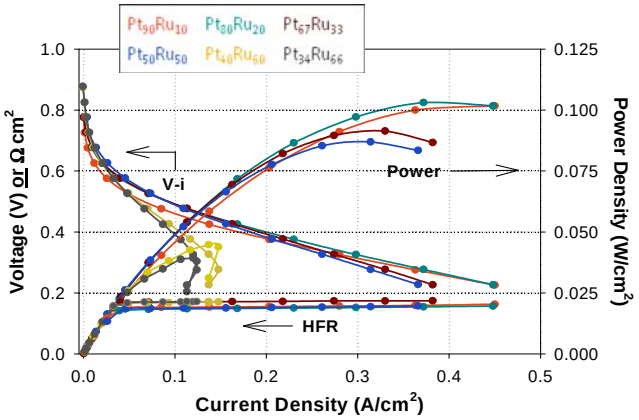


**Figure 2.** DDMEFC performance with different PtRu anode catalysts; anode: 6 mg/cm$^2$ PtRu, 40 sccm DME gas, 30 psig; cathode: 4 mg/cm$^2$ Pt, 500 sccm air, 20 psig; membrane: Nafion® 117; cell temperature: 80ºC.

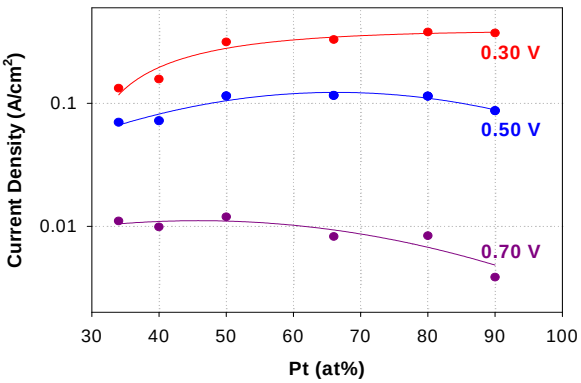


**Figure 3.** DDMEFC current density as a function of Pt content in the PtRu black catalyst.

## DME Anode Activity and Fuel Crossover

DME anode polarization and crossover plots in comparison with those of methanol are presented in **Figures 4a** and **4b**. It is evident in Figure 4a that the onset potential of DME electrooxidation is higher than that of methanol, implying that in the low potential region, the adsorption rate of DME on Pt or the formation rate of the intermediate adsorption species is slow compared to methanol. Meanwhile, PtRu anode deactivation towards DME oxidation is found to occur at high potentials, likely due to the surface oxide formation (more oxophilic and thus less active surface). Fuel crossover experiments (Figure 4b) reveal much lower DME oxidation current at the cathode than that of methanol, especially at higher potentials, indicating lower DME crossover and, again, inactivity of the oxidized Pt (Ru-contaminated (20)) cathode surface in DME oxidation.

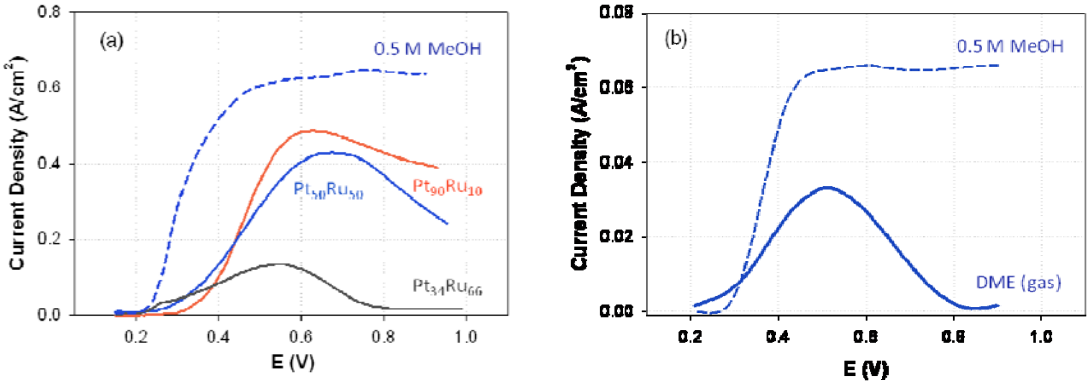


**Figure 4.** (a) Anode polarization and (b) fuel crossover plots of the DDMEFC and the DMFC. anode: 6 mg $cm^{-2}$ PtRu black, 40 sccm DME, 30 psig or 6 mg $cm^{-2}$ $Pt_{50}Ru_{50}$ black, 0.5 M MeOH, 1.8 mL $min^{-1}$; cathode: 4 mg $cm^{-2}$ Pt black, 20 psig, 200 sccm $H_2$ (anode polarization) or 200 sccm $N_2$ (crossover); membrane: Nafion® 117; cell temperature: 80ºC.

## Half-Cell Electrochemical Measurements

The cyclic voltammograms for DME electro-oxidation at a Pt black modified glassy carbon electrode in electrolyte solution with and without saturated DME in the potential range from 0.05 V to 1.2 V are shown in **Figure 5a**. The CV without DME in the potential range from 0.05 to 0.4 V corresponds to the hydrogen adsorption-desorption region. However, the peaks in the hydrogen region in the presence of DME are significantly suppressed because the Pt sites are poisoned by the adsorption intermediates formed in the DME electrooxidation. During the positive-going scan, no significant oxidation current is observed up to 0.5 V. Two evident peaks appear between 0.7 and 0.8 V, which are correlated to the oxidation of adsorption intermediates. These two peaks have been attributed to the oxidation of $CO_{ad}$ and $(–CHO)_{ad}$ by Kerangueven (16) and Zhang (21), but their conclusions are in conflict with each other regarding which peak is related to the oxidation of $CO_{ad}$. No oxidation current is observed above 0.9 V because in this potential region the surface of Pt is gradually covered with the Pt oxides and therefore less active for the DME oxidation (5). This result stands in contrast to methanol oxidation, which continues up to 1.5 V. However, in contrast with Müller's result (2), the CV curves with and without DME above 0.9 V in the positive-going scan are not completely superimposed, indicating that some adsorbed species may be present at the Pt

surface in this potential region and block the formation of Pt oxides. In general, DME does not adsorb as readily on Pt as methanol does. Müller (2) has ascribed this phenomenon to two possible reasons: (i) the second methyl group in the DME molecule renders C-H bonds less reactive compared to those of methanol; (ii) DME adsorption on a surface already covered with reaction intermediate is less favorable from a geometric point of view compared to methanol.

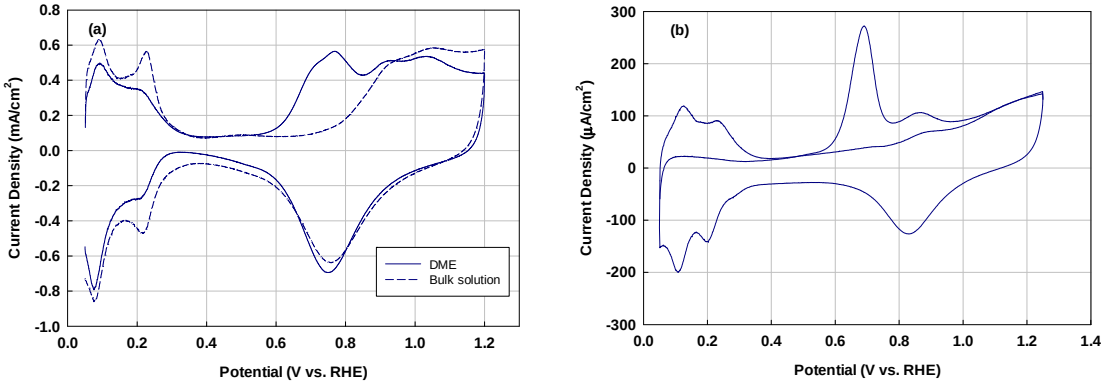


**Figure 5.** (a) CVs of 60 μg/cm$^2$ Pt black in 0.5 M $H_2SO_4$ saturated with DME (solid trace) or without DME (dashed trace) under $N_2$ atmosphere at room temperature. Scan rate: 50 mV/s. (b) Stripping voltammogram of DME. Scan rate: 10 mV/s.

According to the previously published results of *in situ* IR spectroscopic experiments, $CO_L$ is the dominant adsorption species for the DME electrooxidation. It has been demonstrated that the coverage of the adsorption species is ca. 90% for the DME oxidation at $0.1 < E < 0.45$ V. The fractional coverage of $CO_L$ increases with the increase in the potential from 0.1 to 0.4 V and it is larger than 50% at $0.3 < E < 0.5$ V (17). Other main intermediate species include $(CH_3OCH_2–)_{ad}$, $CO_B$, $(–CHO)_{ad}$ and $(–OCH_3)_{ad,}$ which have also been reported by most of the research groups. Additionally, several unique intermediates such as $(HCOO–)_{ad}$, $(CH_3COO–)_{ad}$ and $(CH_3OCOO–)_{ad}$ have been observed by fewer groups, suggesting a complex mechanism of DME electrooxidation.

In order to obtain clearer information concerning the DME adsorption at Pt, a DME stripping experiment was performed (**Figure 5b**). In this experiment, DME is initially adsorbed at 0.25 V in 0.1 M $HClO_4$ solution for 100 s, then it is removed from the solution by bubbling pure $N_2$ for 25 min (the electrode is still held at 0.25 V); finally, the potential sweep is started at 10 mV/s for three cycles to observe the stripping of DME intermediates and to subsequently verify that the DME in solution has been thoroughly removed. The maximum stripping current is obtained at 0.69 V, which can be probably attributed to the oxidation of the same adsorption species as those that have given rise to the first oxidation peak in Figure 5a.

The stripping peak in Figure 5b was integrated in order to determine the quantity of charge involved in the DME adsorption ($Q_{ox}$). $Q_{ox}$ as a function of adsorption time ($t$) and potential are shown in the **Figures 6a** and **6b**, respectively. Figure 6a indicates that $Q_{ox}$ increases with adsorption time within 100 s and becomes time independent after 100 s, demonstrating the DME adsorption has reached a maximum coverage. In Figure 6b, for adsorption potential region 0 to 0.2 V (hydrogen region), $Q_{ox}$ appears to be potential

dependent; in the potential from 0.2 to 0.4 V, the adsorption of DME seems to be potential independent since $Q_{ox}$ is constant with increasing adsorption potential; when potential is higher than 0.4 V, $Q_{ox}$ decreases due to the formation of OH species at the Pt surface leading to the oxidation of adsorbed species associated with DME (16). These results are comparable with those of methanol oxidation at Pt electrodes (22).

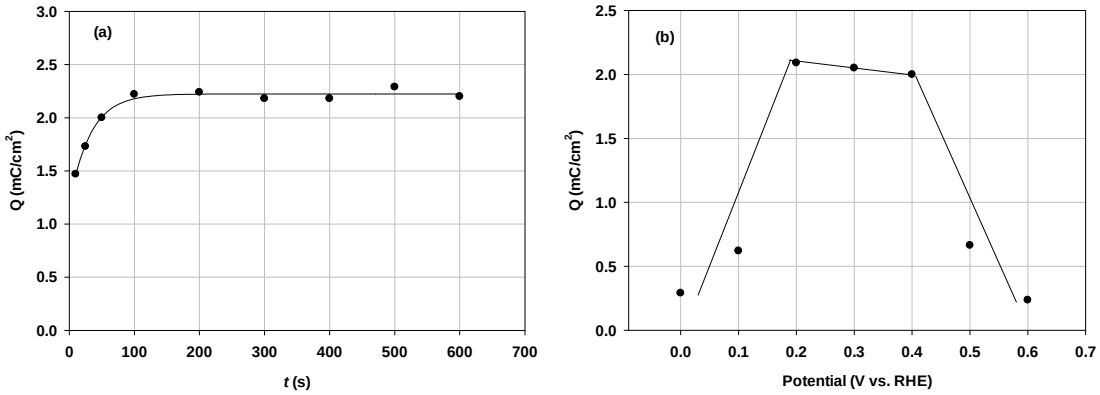


**Figure 6.** $Q_{ox}$ as a function of (a) adsorption time ($t$) and (b) adsorption potential.

## Conclusions

In this study, unsupported PtRu catalysts with a wide range of Pt-to-Ru ratios have been screened for the DDMEFC performance for the first time. Generally, $Pt_{50}Ru_{50}$ have shown the best overall performance in the high and middle voltage ranges and $Pt_{80}Ru_{20}$ has performed the best at low voltages. A maximum power density of 0.10 W/cm$^2$ has been achieved at a current density of 0.37 A/cm$^2$. In spite of using gaseous DME feed (the water supply is insufficient for the complete oxidation of DME at DME gas feed conditions), the measured performance has exceeded the best previously published results. Specifically, Ru-rich catalysts have offered better activity performance at high fuel cell voltages (kinetic region of the anode) and Pt-rich catalysts have performed better at low voltages (near peak power). This effect can be explained by a bi-functional mechanism of DME oxidation, according to which Ru activates the water molecule to generate OH species at low potentials and subsequently oxidize the CO (the dominant intermediate of DME adsorption on Pt) thus reducing the poisoning of the Pt sites. However, initial DME adsorption at Pt requires several adjacent sites, and Ru excess is likely to decrease the surface accessibility for DME.

In addition, we have studied the effects of the DME flow rate and the anode backpressure on the DDMEFC performance and compared the DDMEFC anode polarization and fuel crossover curves with those of a DMFC. Although the DDMEFC suffers less from fuel crossover than DMFC, the electrooxidation of DME is kinetically slower than that of methanol. In half-cell electrochemical measurements, it is shown that DME adsorption at Pt black is less competitive with other adsorbed species such as hydrogen, hydroxyls and oxides than methanol. Meanwhile, the DME adsorption is found to be potential dependent in the hydrogen region of Pt and independent in the double layer region. Although the mechanism of DME electrooxidation has not been completely clarified, the successful development of an advanced electrocatalyst for DME oxidation is the key for the commercialization of a DDMEFC.

## Acknowledgments

Financial support from the DOE-EERE Fuel Cell Technologies Program is gratefully acknowledged.

## References

1. A. Serov and C. Kwak, *Applied Catalysis B: Environmental*, **91**, 1 (2009).
2. J. T. Müller, P. M. Urban, W. F. Hölderich, K. M. Colbow, J. Zhang and D. P. Wilkinson, *J. Electrochem. Soc.*, **147**, 4058 (2000).
3. I. Mizutani, Y. Liu, S. Mitsushima, K.-I. Ota and N. Kamiya, *J. Power Sources*, **156**, 183 (2006).
4. M. Muraoka, Y. Liu, I. Mizutani, A. Ishihara, S. Mitsuishima, K.-I. Ota and N. Kamiya, *J. Hydrogen Energy Syst. Soc.*, **29**, 51 (2004).
5. Y. Liu, S. Mitsushima, K.-I. Ota and N. Kamiya, *Electrochim. Acta*, **51**, 6503 (2006).
6. J.-H. Yoo, H.-G. Choi, C.-H. Chung and S. Cho, *J. Power Sources*, **163**, 103 (2006).
7. G. Kerangueven, C. Coutanceau, E. Sibert, J.-M. Leger, C. Lamy, *J. Power Sources*, **157**, 318 (2006).
8. M. Mench, H. Chance and C. Wang, *J. Electrochem. Soc.*, **151**, A144 (2004).
9. J.-H. Yu, H.-G. Choi and S. Cho, *Electrochem. Commun.*, **7**, 1385 (2005).
10. J.-Y. Im, B.-S. Kim, H.-G. Choi and S. Cho, *J. Power Sources*, **179**, 301 (2008).
11. K.-D. Cai, G.-P. Yin, J. Zhang, Z.-B. Wang, C.-Y. Du and Y.-Z. Gao, *Electrochem. Commun.*, **10**, 238 (2008).
12. K.-D. Cai and G.-P. Yin, *Int. J. Energy Res.*, **34**, 695 (2010).
13. L.-H. Xing, Z.-B. Wang, C.-Y. Du and G.-P. Yin, *Int. J. Energy Res.*, accepted.
14. Y. Tsutsumi, Y. Nakano, S. Kajitani, S. Yamasita, *Electrochemistry*, **70**, 984 (2002).
15. M. Shao, J. Warren, N. Marinkovic, P. Faguy and R. Adzic, *Electrochem. Commun.*, **7**, 459 (2005).
16. G. Kerangueven, C. Coutanceau, E. Sibert, F. Hahn, J.-M. Leger and C. Lamy, *J. Appl. Electrochem.*, **36**, 441 (2006).
17. Y. Liu, M. Muraoka, S. Mitsushima, K.-I. Ota and N. Kamiya, *Electrochim. Acta*, **52**, 5781 (2007).
18. Y. Zhang, L. Lua, Y. Tong, M. Osawa and S. Ye, *Electrochim. Acta*, **53**, 6093 (2008).
19. H.A. Gasteiger, N. Markovic, P.N. Ross, E.J. Cairns, *J. Electrochem. Soc.* **141** 1795(1994).
20. P. Piela, C. Eickes, E. Brosha, F. Garzon, P. Zelenay, *J. Electrochem. Soc.* **151** A2053 (2004).
21. Q. Zhang, Z. Li, S. Wang, W. Xing. R. Yu and X. Yu, *Electrochim. Acta*, **53**, 8298 (2008).
22. B.J. Piersma and E. Gileadi, in J.O'M. Bockris (Ed.), *Modern Aspects of Electrochemistry*, Vol. 4, Ch. 2., (Butterworths, London, 1966), pp. 102.